Available on CMS information server

CMS NOTE 1997/036

The Compact Muon Solenoid Experiment

CMS Note

Mailing address: CMS CERN, CH-1211 GENEVA 23, Switzerland

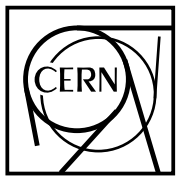

May 5, 1997

Studies and Proposals for an Automatic Crystal Control System

G. Drobychev[1,2], A. Fedorov[1], M. Korzhik[1],
A. Khruschinsky[1], O. Missevitch[1], J.P. Peigneux[2],
A. Oriboni[2], M. Schneegans[2]

1. INP Institut for Nuclear Problem - MINSK (Belarus)
2. LAPP Laboratoire d'Annecy de Physique des Particules - (France)

Abstract

This document presents the status of the studies for an Automatic Crystal COntrol System (ACCOS) performed since autumn 1995 for the CMS collaboration. Evaluation of a start–stop method for light yield, light uniformity and decay time measurements of $PbWO_4$ crystals is presented, as well as the first results obtained with a compact double-beam spectrophotometer for transverse transmission. Various overall schemes are proposed for an integrated set-up including crystal dimension measurement. The initial financial evaluation performed is also given.

1. Introduction

2. Purpose of ACCOS

2.1 Scintillating crystal properties to be certified
2.2 Optical transmission measurements: methods and instruments
2.3 Possible methods of scintillation parameter measurements and related quantities.
2.3a Pulse-height spectra measurements using radioactive source, cosmic rays, microtron, etc.
2.3b Single-photon counting

3. Integrated system of scintillation element certification

3.1 Main algorithms and methods
3.1a Dimension measurements and identification of crystals
3.1b Optical transmission measurements
3.1c Decay time: LY and LY uniformity measurements
3.2 Physical structure of the system

4. Current status of implementation

4.1 Hardware
4.1a Dimension measurement system, bar-code reader, and moving platform
4.1b Optical spectrometer OS-1 prototype
4.1c Decay time and LY spectrometer prototype
4.2 Software
4.3 Schedule and cost

Appendix 1 Algorithms of data collection and calibration

A.1 Optical transmission measurements:

Reconstruction of the longitudinal transmission and transversal transmission non-uniformity, calculation of the light attenuation length.

A.2 Decay time curve processing:

Corrections for instrumental factors.

A.2.1 Source decay

A.2.2 Dead-time losses and distortion

A.3 LY uniformity curve processing:

Correction for deposited energy and spatial function of excitation. Correction for solid angle, visible by 'stop' photodetector. Correction for difference in absorption length visible by PM and APD.

Appendix 2 Decay time and light yield measurement – Results

Appendix 3 Transmission measurement with OS-1 – Results

Appendix 4 Crystal dimension measurements and mechanical installations. Some policy considerations.

References

1. Introduction

This document presents the status of the studies for an Automatic Crystal Control System (ACCOS) performed since autumn 1995 for the CMS collaboration.

The essential parameters of more than 100 000 $PbWO_4$ (PWO) crystals should be measured and reliable information recorded in a database. Laboratory methods used until now for a rather limited amount of channels (up to 10^4) should be given a more automatic and industrial approach. The present studies have attempted to take this aspect into account and solutions to achieve this aim are proposed. Measurements of different parameters are given as well as specific methods and studies for carrying them out. The evaluation of the main parts of an ACCOS system was made by LAPP (Annecy) and the INP (Minsk) team, in collaboration with CERN.

Throughout this paper the following abbreviations will be used:

ACCOS – Automatic Crystal COntrol System
APD – Avalanche Photo Diode
ECAL – Electromagnetic Calorimeter
ESS – Energy Scale Stabilization system
LY – Light Yield, measurement of scintillation and collection efficiency
LYN – Light Yield Non-uniformity
PC – Production Centers
PD – Photo Diode
PM – Photomultiplier tube
PWO – Lead tungstate scintillating crystal $PbWO_4$
RC – Regional Centre
RH – Radiation Hardness (measurement of LY change under irradiation).

2. Purpose of ACCOS

The aim of the present work is to design an automatic system for the certification of the ECAL PWO crystal properties (dimensions, optical and scintillation characteristics, and other properties which could be inferred from these measurements). The studies were conducted bearing in mind that several similar machine exemplars will ensure the basic measurement requirements near the production and regional centres with a high productivity. They will provide a complex set of permanent routine measurements for efficient output delivery in PCs and for input reception in RCs, having in mind minimization of crystal manipulation and of the rejection rates of unwanted crystals at RCs. One of the important functions of the ACCOS system is the unification all over PCs and RCs of the certified parameters by using identical methods and apparatus to deliver data to customers in a unified database in the frame of the so-called C.R.I.S.T.A.L. program [1]. Last, but not least, reliability and minimal cost have been taken into account as much as possible once the scientific and technical needs were fulfilled.

The system was elaborated in a modular way, associating as much as possible standard elements which can be purchased in industry and specific items dedicated to special operations which are inserted in a way to be easily removed or replaced. Furthermore, additional instruments can be integrated into the system when complementary measurements are required. However, laboratory research instrumentation should be used separately for specific and more detailed studies.

The ACCOS productivity level should match the output control needs of the most powerful crystal suppliers – Bogoroditsk Techno Chemical Plant (Russia) and the Shanghai Institute of Ceramics (China). Thus, the ACCOS systems installed there should be able to process up to 60 crystals a day. On the other hand, they should be able to execute measurements automatically on a 3×8 h basis, with minimum human intervention, except for loading and unloading the crystal batches. It should also fulfill the productivity needs of the Regional centres which may receive crystal batches from several producers at a time.

As a consequence, the ACCOS system must be designed in such a way that it is easy to use and can be operated by a minimal amount of technical staff. The system installation should not require additional expenses on areas, such as special engineering for radioactive, laser or chemical security requirements, etc. Additional expenses for extra engineering work, additional equipment and maintenance staff (radiation safety services, not enough automatisation, etc.) will contribute to the final crystal cost. For the same reason, the ACCOS system will not contain expensive equipment such as multipurpose luminescence spectrometers, monochomators, X-ray pulse sources or microtrons, etc., all of which can be used, if available, for complementary measurements.

2.1 PWO crystal properties to be certified

At present, the most important PWO crystal parameters to be certified are as follows :

The PWO crystal dimensions should be in agreement with the specified tolerance. The crystals are truncated pyramids with trapezoidal end faces. Their dimensions are characterized by the length and by 3 numbers for each end section which have to be compared to nominal values. Since crystal edges are not perfectly defined (chamfers), the safest way is to measure the space coordinates of a set of points of each crystal face and derive the equation of the plane. The planarity of each face can be checked as well as the angles between faces. The intersections of the planes will yield the wanted dimensions. The precision desired on dimension measurements is $\approx \pm 5$ μm in order to obtain distributions which can be well situated in the tolerance interval.

Light yield (LY): a measurement of the transformation efficiency of ionizing radiation energy to the energy of light photons visible by PM or APD. The LY expressed in photoelectrons per MeV corresponds in fact to the light produced and collected at the face coupled to the photodetector.

Light Yield Non-uniformity (LYN): relative change of LY along the scintillation element. Usually, this is a plot of LY values measured at several points (10 or more) along the crystal. This parameter has a significant influence on the energy resolution of the PWO detecting cell. LYN can be expressed in percent.

Scintillation Kinetics: a function, curve, histogram or data file describes the change of the scintillation light yield value with time after excitation. This usually involves recording the shape of the scintillation pulse by a specific method. Using the parameters of the scintillation pulse, it is possible to determine the amount of light collected in a specified time gate and evaluate the probability of pile-up for a specific detector count rate. The parameters of the scintillation kinetics can be presented as decay times of the scintillation light components and their amplitudes, or as a number of scintillation photons emitted in specified gates. At the producer facilities, scintillation kinetics should be measured with a sensitivity to slow

components several times better than the requirements in the final crystal specifications. This is made necessary by the increase of the slow components from crystallization to crystallization, taking into account that at least two batches of crystal are grown during the time between crystal growth and the first measurement.

Optical Transmission Spectra

- **Transversal transmission:** the spectra are measured transversally in about 10–20 points along the scintillation elements. These data are necessary in order to check transmission non-uniformity which may be caused by technology deviations or quality of the raw materials. This feature will allow bad crystals to be rejected and possibly the radiation hardness of the crystals to be predicted.
- **Longitudinal transmission** is used to detect possible wide absorption bands and to determine the light attenuation length of the scintillation spectrum. This parameter is useful for the uniformization of the light collection of the scintillation elements.

Optical quality check: this is a standard procedure for selecting crystals without macroscopic defects such as bubbles, milky defects, etc. Usually this operation is performed visually, but it could be implemented using modern compact high-resolution image digitizer (CCD camera plus ADC plug-in card) and image processing software (which has been well developed for radiolocation problems). Such an automated set-up would significantly improve the reliability of these data and decrease manipulation of the crystals, according to the aims of ACCOS.

Radiation Hardness: no reliable correlation has been observed yet between the radiation hardness and the PWO parameters studied in laboratory conditions. However, it is not possible to measure the radiation damage of each PWO element delivered because of the cost and human resources involved. The radiation hardness of some crystals from different batches should be tested in detail, whereas others should be evaluated by routine certification measurements and their correlation with radiation hardness if established.

R&D on the origin of radiation damage in PWO and on the improvement of radiation hardness is still ongoing. This R&D should hopefully result in the establishment of a stable correlation.

2.2 Optical transmission measurements: methods and instruments

The optical transmission of PWO scintillating elements will be certified at least in the range 300–700 nm for the evaluation of:

a) non-uniformity of the transmission,
b) light attenuation length,
c) LY Non-uniformity minimization by wrapping, painting, etc.,
d) data correlated with crystal parameters such as radiation hardness, which could then be predicted with high reliability.

If the dimensions of the PWO elements are ***a, b, c;*** and $\boldsymbol{a \cong b < c}$, where ***c*** is the length of the scintillator and ***a, b*** is its height and width, then two possibilities for the transmission measurements exist. The first one is the longitudinal transmission measurement which gives the spectrum of the transmission through a 23 cm long crystal. The second is the transversal transmission measurement at several points along ***c*** direction. There are both advantages and drawbacks to these methods.

Longitudinal transmission measurement can be implemented with commercially available spectrometers, but requires an expanded sampling chamber and additional optics in order to improve light beam divergence as well as a good crystal positioning system. The spectrum obtained in this way provides data for the calculation of absorption attenuation length at any wavelength from the selected region. It shows the short wavelength cut-off of the spectrum that brings information about possible defects and impurities present in the crystal. However, the data obtained from such a measurement do not contain any information about the non-uniformity of the crystal transmission along the ***c*** side. Furthermore, this method does not allow defects in the crystal such as bubble corners or other scatters, which sometimes exist in the initial or tail part of the crystal, to be identified.

On the contrary, the transversal transmission measurement can provide information about the non-uniformity of the transmission and additional information necessary to uniformize crystal light collection with APD, using LYN data obtained with PM readout (Light Yield Non-uniformity data should be corrected taking into account the difference between PM and APD spectral response).

In principle, longitudinal transmission can be reconstructed using transversal transmission data. However, for PWO scintillation elements it is impossible (as shown in Appendix 1) to obtain the necessary precision and therefore both type of transmission measurements should be performed.

Methods using two or one light beam can be used for transmission measurement. The double-beam method has a definitive advantage: it suppresses multiplicative errors caused by the drift of light source parameters and is more suitable for permanent certification measurements of PWO crystals at the mass production stage.

As PWO is a birefringent crystal and the shape of the scintillation elements varies, a precise positioning of the light testing beam and photodetector is required. In particular, methods based on Photo-Diode arrays for registration are not reliable for either longitudinal or transversal transmission routine measurements.

The transversal transmission measurement at several points along the crystal lasts longer than longitudinal transmission measurement, when equipment with a standard system for the wavelength scan is used. To overcome this disadvantage, it is necessary to use advanced measurement techniques.

The PWO transmission spectrum does not have singularities like the spectra of crystals doped with rare earth ions, so different schemes of wavelength selection for its routine transmission measurement are acceptable. Moreover, it is not necessary to measure the PWO transmission spectrum at many wavelength points. It can be measured at several properly chosen wavelengths only with subsequent reconstruction of the total spectrum. In this way, higher speed in the measurements will be achieved. For this purpose, a rotating wheel with interference filters can be used and the double-beam method with light-beam modulation in time yields sufficient accuracy, when a small and convenient photodetector such as a PD is used. To achieve this goal, a portable double-beam spectrometer based on a set of interference filters with an UV–extended PD has been developed. The parameters of the device and its design are described below (see 4.1b).

2.3 Possible methods of scintillation parameter measurements and related quantities

The dependence of 2% $^{\circ}C^{-1}$ of PWO LY on temperature [2] implies that temperature of the PWO crystal must be well controlled during the LY measurement process. Temperature stabilization is also needed for the dimension measurement process, but to a lesser extent: typically, the warranted precision is given for a 1°C stabilization range. For LY measurement process at least time of stabilization is foreseen during the measurement of the preceeding crystal batch in the

measurement cabin (see Appendix 4). The relative precision of the LY measurement by the start stop method, as it is used here, is dominated by the statistics and would reached a $\sigma \approx 1\%$.

2.3a Pulse-height spectra measurements using a radioactive source, cosmic rays, microtron, etc.

With such methods, LY and LYN can be measured using the spectrum shape or the positions of the peak with appropriate fits and extrapolations if necessary. For instance, the total photoabsorption peak position N_{Co} in the pulse-height spectrum of a ^{60}Co isotope, if resolved well enough from the Compton events and the PM noise, is proportional to the light yield: $LY = C*N_{Co}$, where C is a calibration coefficient.

Owing to the relatively small PWO light yield (5–20 ph.e./MeV, i.e., 6–24 photoelectrons in the ^{60}Co peak of total absorption), reflective and diffusing wrapping of the crystal and optical coupling between crystal and PM are essential. These requirements significantly decrease the flexibility and speed of the measurements and bring additional systematic uncertainties.

High-energy charged cosmic particles could seem to be a simple and inexpensive option. Their energy deposition around 20–30 MeV should make possible the APD readout application. However, LY and scintillation kinetics information (by digitizing the pulse shape) cannot be extracted from the amplitude and shape of a single particle (even from the PM-recorded scintillation pulse) with required precision. Unfortunately, the intensity of muons and mesons is rather low: about 200 $s^{-1}m^{-2}$ in an effective solid angle of 40–50°. The PWO element side area can be taken as 40 cm^2 for averaged LY and kinetic measurement, and as 1–2 cm^2 for LYN recording. Taking into account that the energy deposition is proportional to the length of the particle trajectory in the crystal, a narrow solid angle ($\approx 8°$) should be chosen by trigger counters in order to provide a difference in the particle trajectories of less than 1% (typical requirements on LYN determination).

As a result, a cosmic-ray-based system will either contain numerous position-sensitive trigger detectors (at least, 2 linear arrays) with further computerized reconstruction of trajectory length and interaction point coordinates to avoid losses of events intensity, or it will be unacceptably slow ($\approx$ 0.5–1 hour per single point) in operation when based only on two trigger counters.

When a pulse of an X-ray source is used for the crystal excitation, depending on pulse duration and source intensity, both light yield and pulse shape can be measured with PM, or even with APD readout. In this case an instrument such as a digitizer can be used, and the digitized signal can be fitted to a chosen mathematical function. When this approach is used, the time resolution is limited by the duration of the X-ray source pulse, the width of the PM response to a single photon (typically 5 ns), or the APD time response. The output energy of an X-ray source pulse is the sum of single X-ray photon energie (about 100 KeV typically). The interaction of these photons with the heavy PWO scintillator will occur mostly at its surface layer. This makes this method more sensitive to the quality of the crystal surface, and to the conditions of polishing and annealing when LY and LYN are measured.

Methods using high-energy gamma quanta or particles from microtron or proton sources, etc. are probably the most reliable for LY and LYN measurements. Whilst pulse digitizing is used for determination of scintillation kinetics parameters, the time resolution limits described above also play a role.

In addition, pulsed X-ray sources, microtrons, etc. are expensive devices and can hardly be used for routine certification measurements only. All pulse-height measurements require high stability of the spectrometric chain. High voltage and amplifier gain instabilities will both result in a shift of the spectrum peak positions. Therefore, thermostabilization of the crystal measurement

chamber and of the light or electrical reference signals for the spectrometric chain monitoring, must be used.

2.3b Single-photon counting

The method of photon counting is well known as a method for weak light signal measurement in optical spectroscopy. Methods of scintillator light yield measurement by photon counting also exist. In this case, the scintillation light is attenuated down to a level where the single photon PM pulses are separated in time without pile-up. Then, the count rate in the presence of scintillation light is measured. It is proportional to the scintillator light yield if the background ('dark') count rate is substracted.

Similar solutions are used in the so-called 'start-stop' method, or [3, 4] widely used for scintillation decay time measurements. The decrease of the scintillation amplitude with time results in an increase of the average time between irradiation by individual photons. Therefore, the delayed coincidence method measures the arrival times of individual photons after initial excitation. A constant fraction discriminator (CFD) generates accurate time markers, and the time difference between the excitation and the individual photon arrival time is measured by a time-to-digital converter (TDC). Using an annihilation γ-quanta source like ^{22}Na which emits simultaneously two 511 keV gamma-quanta in opposite directions, one of them can generate a time marker of the excitation in a start–channel, whilst the second one excites scintillation in the investigated specimen (Fig. 1) which is detected in the stop channel.

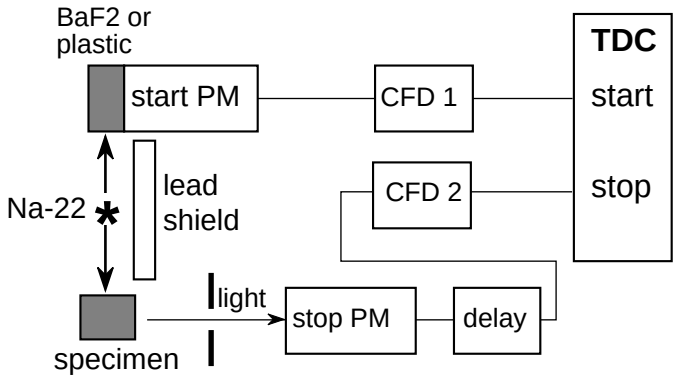

Fig. 1: Typical configuration of the delayed coincidence method.

This method improves the timing resolution significantly in comparison with the pulse digitizing methods. The timing uncertainty is caused by the timing jitter of the PM (typically 100–300 ps), the CFD (100–200 ps), and by the TDC resolution (25–50 ps). The timing uncertainty caused by the annihilation gamma-quanta escape from the positron ^{22}Na source is negligible.

The start-stop method puts two constraints on the event rate, which establish the limits of productivity. One is the limitation of the annihilation source activity. It should not exceed ~10^5 Bq. At higher activity the probability of random coincidence of two gamma-quanta from different decays (background) becomes too high. The second is the limitation of the probability to detect photons in the stop channel per single excitation. The most widely used one-hit TDC requires an average number of detected photons of not more than 0.1 per single excitation; otherwise the measured scintillation decay curve will be distorted, especially in the slow component region. The stop channel detector dead time can also cause distortion, but only in the fast component region. Two types of advanced TDC, the multi-hit TDC and the one-hit TDC with a multi-stop rejection unit, were developed to overcome distortion problems. The multi-hit TDC can measure the arrival

time of several scintillation photons resulting from a single excitation. This increases measurement productivity. The one-hit TDC with multi-stop rejection cancels conversion when more than one 'stop' photon arrives within the full time scale after excitation. A short comparison of all three types of TDC can be found in Ref. [4]. A more comprehensive analysis of the TDC with multi-stop rejection is made in Ref. [5]. The general conclusion reached from these studies is that the multi-hit TDC is the best method when the fastest component of scintillation is much longer than the dead time of the stop channel (this is not the case for the PWO) and the one-hit TDC with multi-stop rejection unit is the best when the fastest component in scintillation is less or comparable to the stop channel dead times (as with PWO scintillators).

When the delayed coincidence method for scintillation decay time measurements is applied, the proportionality between the stop channel count rate and the scintillator light yield can be used to determine LY from the decay spectrum. This means that the scintillation decay times and the light yield of a scintillator can be measured simultaneously. In this case, neither optical coupling between the scintillator and the PM nor scintillator wrapping are needed. The accuracy of LY measurements can be provided by monitoring or stabilization of the start and stop-channels.

3. Integrated system of scintillation element certification

3.1 Main algorithms and methods proposed

3.1a Dimension measurements and identification of crystals

Each crystal should be unambiguously identifed. This can be done by a bar code printed with indelible ink on the crystal or on a plastic label which serves at the same time as a position key. The size of this code could be less than 8 mm high on the 23 mm wide side of the crystal. An automatic bar-code reader, commercially available, will be installed and connected to the database recording software.

The dimension measurements will be made by a standard 3D machine available on the market and its associated software. Worldwide companies able to provide services and warranties all over the world during the whole production period have been investigated. The software available for the 3D machine will also be taken into account, particularly with respect to the ease of access, and to its possibly inclusion in an external automatic program of measurements. More detailed information is provided in Appendix 4.

3.1b Optical transmission measurements

The regular transmission spectrum of PWO crystal consists of a plateau in the 400–700 nm range and a rapidly decreasing transmission curve in the region below 400 nm. The following sampling wavelengths have been chosen for the transmission measurement: 319, 328, 340, 364, 373, 400, 420, 440, 500, 600, and 700 nm. The measurement of the transmission at these selected wavelengths is sufficient to reconstruct the transversal transmission curve with an acceptable accuracy. For this purpose we have built a compact spectrometer in which the wavelengths mentioned above are selected by interference filters. The transversal transmission of a certified scintillation element is measured at **m** points along the crystal. The absorption coefficient **k** for one wavelength can be found from the equation:

$$\mathbf{T_m(\lambda_i) = (1 - r)^2 \times e^{-k_m(\lambda_i)\, l}} \quad , \qquad (1)$$

hence

$$\mathbf{k_m(\lambda_i) = \ln [1 - r (\lambda)]^2/l_n - \ln T_m(\lambda_i) / l_m,}$$

where

m is the point number along the crystal;

$\mathbf{k_m(\lambda)}$ is the absorption coefficient for the point **m** at the (λ_i)wavelength;

$\boldsymbol{l_m}$ is the transversal dimension of the crystal at point **m**;

$\mathbf{r(\lambda_i) = [n(\lambda_i) - 1]/ [n(\lambda_i) + 1)]^2}$ and $\mathbf{n(\lambda_i)}$ is the refractive index at λ_i of the ordinary beam;

$\mathbf{T_m(\lambda_i)}$ is the measured transmission at λ_i at point **m.**

The value of $\boldsymbol{l_m}$ is determined as

$$\mathbf{l_m = a \times \cos \alpha + (x + a \sin \alpha) (\cos^{-2} (2\alpha) -1)^{1/2}} \qquad (2)$$

where

a is the height of the top surface of the scintillation element;

x is the distance between the point **m** and the top surface;

α is the tapering angle as shown in Fig. 2:

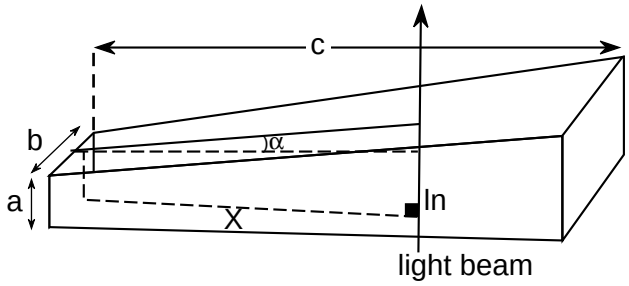

Fig. 2: Transversal transmission measurement geometry.

The light beam is perpendicular to the entrance side of the crysta
beam deviation caused by the refraction.

The valuekofs used to reconstruct and plot the transmission curve in
of the certified scintillation element as well as to compute the tra
uniformity and to make the correction for the different spectral respor
These equations are presented in Appendix 1.

3.1c Decay time: LY and LY uniformity measurements

For the simultaneous measurements of the scintillation kinetics, the scintillator light yield and the light yield non-uniformity, the method of delayed coincidences has been chosen. An appropriate number of points for LYN measurements would range from 10 to 20, and the time duration for one–point measurements should not exceed 1–2 min with a one-hit TDC and 20 s with a multi-stop rejection unit. The experimental configuration which meets these requirements is usually similar to the one described in 2.3b, and differs mainly in geometry of the scintillator start and stop channels (Fig. 3) where the ^{22}Na source slides along the crystal face at a constant 2–3 mm distance. Two stabilization systems in both the start and stop channels are used.

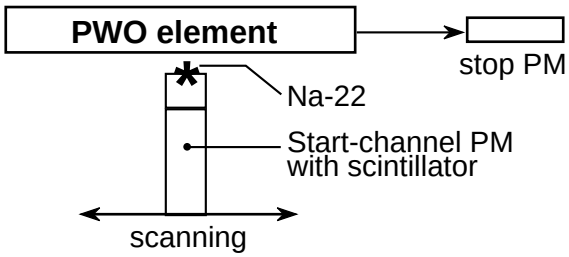

Fig. 3: Geometry of the scintillator start and stop channels.

An algorithm for the experimental decay curve processing has been developed and can be summarized as follows:

a) As shown in Fig. 4, the background level of the random coincidences is determined in the Region Of Background (ROB) by averaging the channel content.
b) The integral of the kinetics spectrum (with the background subtracted from the channel contents) is taken in the preselected Region Of Interest (ROI). Both the ROB and ROI settings are stored in a configuration file and do not change during the measurements of different crystals.
c) A measured distribution is fitted to the monoexponential function $\mathbf{y = A \times exp\ (-t/\tau)}$ on the right half of the ROI where the contribution of fast components is negligible. The fitting procedure uses the non-iterative method of the two integral ratio, which was most stable with poor statistics. The output results of fitting are the amplitude **A** and the decay-time constant τ of the slow component.
d) The time, during which 99.9% of the light is collected, is determined within the TDC scale or extrapolated.
e) The crystal LY is given for 99.9% light collection time.
f) The values of LY in photoelectrons or percent are given for several time gates (normally five, i.e. 30, 50, 100, 200, and 1000 ns) starting from the moment of excitation.
g) The protocols of measurements at several points along the crystal are saved in a file.
h) The LY non-uniformity curve (LY value for predefined time gate vs coordinate) is plotted by taking the data from a file. The correction of this curve for instrumental factors and for the APD spectral response is performed as described in Appendix 1.

Such a presentation does not contain decay times and amplitudes of exponential components in PWO decay. However, it is possible to observe directly how much scintillation light will be collected within a specific time gate, and how large the drift of the baseline due to pile-up (readout detector constant current) will be. This information is especially important for the user.

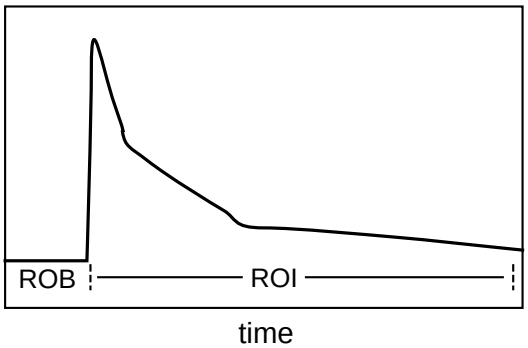

Fig. 4. Log of decay curve.

3.2 Physical structure of the system

The proposed ACCOS system would be built around a 3D machine for the dimension measurements, equipped with a server able to carry as much as 20 crystals (including a reference one) for the five basic operations foreseen today:

a) Crystal identification with a bar-code reader.
b) Crystal dimension measurements with sensors (such as a Renishaw PH6 head) mounted on a standard 3D machine as small as possible according to what is available on the market.
c) Transversal optical transmission measurements at several points along the crystal with a specially designed compact double-beam spectrophotometer.
d) Longitudinal optical transmission.
e) Measurements of LY, LYN and scintillation kinetics under γ irradiation can be performed with the spectrometer on the basis of a ^{22}Na annihilation source, through one set of measurements.

Data will be acquired, processed and stored in a computer workstation (i.e. a PC) and the Certification Protocol will be generated. The expected certification time for a 20–crystal batch should not exceed 4 h (≈ 10 min per crystal). This would allow at least 3 batches per day to be processed, as initially specified.

The most compact geometry is foreseen with a rotating server carrying the 20 crystals radially with the various measuring set-ups installed along crystals of the server and operating in general one after the other.

This geometry was found to be the most suitable one, fitting both the different constraints of availability on the market and the requirements for compactness, automatics and temperature stabilization. The whole machine is then enclosed in an isolated cabin, which will be easy to build and control for temperature and light insulation, allowing both LY and dimension measurements without temperature change of the crystal. Storage inside the cabin of the next crystal batch under the same temperature conditions is also foreseen (see Appendix 4).

If some functions have to be relaxed (i.e. dimension measurements made only at the production place, ...) other combinations of elements can be foreseen using the same basic elements which have been designed to be as modular as possible. Nevertheless, it must be kept in mind that full functionalities, if scattered, will cost as much or more than the compact system proposed. Other configurations are discussed in Appendix 4. A reference crystal will be installed permanently on the machine and remeasured each time with the current batch in order to check the stability of the measurement process as well as to cross-check the measurements provided by other similar ACCOS set-ups. The parameters of the reference crystals on each ACCOS machine will be carefully measured by sophisticated laboratory methods before being measured and definitively installed on it. This will, in particular, provide the calibration in phe/MeV for the light yield.

4. Current status of implementation

4.1 Hardware

4.1a Dimension measurement system, bar-code reader, and moving platform

During the studies, taking into account the relative softness of the crystal, several means of dimension measurements have been investigated such as interferometry, capacitive comparator, video-image analysis, one-dimensional laser sweep, and mechanical three-dimensional machines. At present, the state of the art of the 3D mechanical machines makes them the most attractive with

respect to precision, speed and reliability of measurement, as well as in terms of price and maintenance.

The machines investigated have a minimum volume of measurement of $700 \times 450 \times 450$mm for the smallest and a maximum of $1000 \times 700 \times 500$ mm for the largest, which is quite sufficient for crystal dimension measurement purposes. They may be equipped with a rotating *plateau* which can serve the dimensional measurement area, whilst the free radii of the plateau can be equipped with optical spectrometers to measure light yield and transmission (transversal and/or longitudinal).

Usually, two types of 3D mechanical measuring machines are encountered: open geometry and closed geometry. The latter is a portico structure for displacing the measuring head, which limits the access to the measurement area in some directions. Nevertheless, both of them can be accommodated with a rotating server, the diameter of which ranges from 920 to 1250 mm.

The rotating server can form part of the 3D machine delivered by the machine constructor with the driver software included. This increases the machine's cost, but gives serious advantages with respect to warranty and synchronization with the measurement processes. It also means that it will be built to the same quality standards as the 3D machine itself. External solutions can be adopted provided that proper agreement is found with the constructor concerning malfunctioning due to a failure of an external part and the incidence of the precision of the machine measurements.

Usually static equipment is easy to install on the measurement platform. A bar-code reader of high quality will be installed on the platform in order to identify the crystals before any measurement process. Bar-code readers as small as $40 \times 50 \times 28$ mm are commercially available and are able to read bars as thin as 0.128 mm, which will allow a rather complete information set (still to be precisely determined) to be fitted on the 23 mm side width of the crystal. It is also possible to connect several bar-code readers to the same computer if scattered in space measuring devices are needed or parallel measuring protocols are foreseen.

4.1b Optical spectrometer OS-1 prototype

A special double-beam portable spectrophotometer for transversal transmission measurement has been designed and built. The optical part of the spectrophotometer includes a 20 W halogen lamp, a four-lens collimator, two objective lenses, an achromatic light beam splitter, a set of interference filters, collecting mirrors in the measuring and reference channels, an UV-extended photodiode (the scheme is shown in Fig. 5), and electronics for the signal amplification (current-to-voltage converter) and ADC reading synchronization. The spectrometer's dimensions are $70 \times 80 \times 220$ mm^3.

The measuring procedure is as follows. The rotating wheel with interference filters crosses in sequence the reference light beam and the information channels. When the non-transparent zone of the wheel crosses the beam, the level of 'dark' signal (depending mainly on the photodiode dark current) is measured. The wheel rotates at about 3000 rpm (50 rotations per second). Such a system provides a fast switching of the light wavelength. After the reference beam passes through the filters, and the information beam passes through the filters and crystal, two spherical mirrors send the beams to the PD working in photo-current mode. A precision low-noise current-to-voltage converter transforms the PD photo-current into a voltage signal, which goes through a fourth order low-pass filter to a 4K channel ADC, triggered by the synchronization scheme, which digitizes this filtered output voltage during the time when the interference filters or non-transparent zones cross the beam. The time necessary to measure the transmission spectrum in the range 319–700 nm is less that 10 sec for one spatial point. As usual, one channel is used for the transmission measurements of the samples (PWO crystals with a variable thickness of 23.8–20.5 mm in our case), and the other channel (the reference one) is used to correct the drift of the lamp intensity,

spectrum and photodetector parameters. The OS-1 spectrophotometer prototype also includes a mechanical platform which is PC-controlled and provides spectrophotometer movement along the crystal.

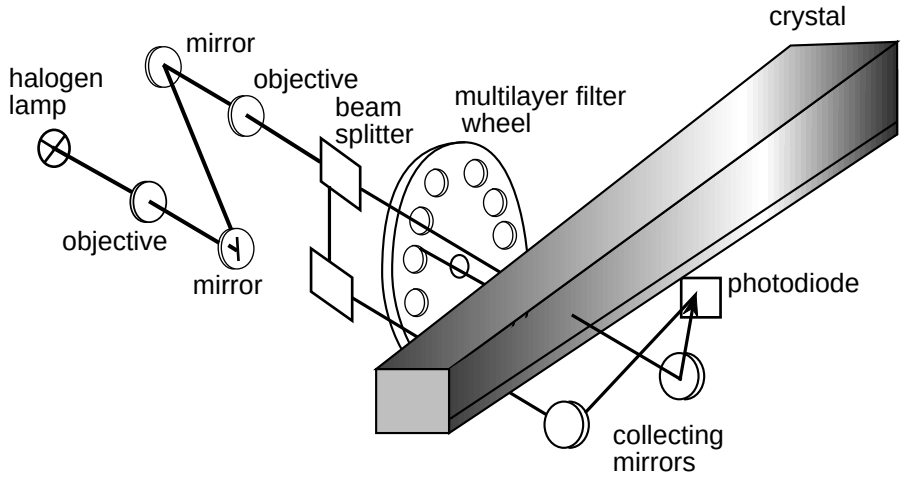

Fig. 5: Double-beam spectrophotometer scheme.

4.1c Decay time and LY spectrometer prototype

A prototype of a delayed coincidence spectrometer has been developed and tested. The general structure of the spectrometer is similar to the one presented in Fig. 1, and the detector section is shown in this Fig. 3. The start-channel detector consists of a Hamamatsu R5900 metal-can type ($28 \times 28 \times 20$ mm) PM coupled to a $\varnothing\ 40 \times 40$ mm plastic scintillator (to be replaced soon with BaF_2). The ^{22}Na annihilation source, with a current activity of 200 kBq, is mounted as close as possible to the scintillator and delivers about 22 000 start signals per second. These, as well as the stop channel count rate are monitored by scalers. The start PM with its scintillator is mounted on a moving platform for scanning along the crystal. This movement can be combined with that of the spectrophotometer.

The stop channel of the spectrometer is based on an ultra-compact low-noise Hamamatsu R5600 PM with single photoelectron dark count rate of 17 cps (selected unit, 80 cps typically). The distance between the stop-PM and crystal bottom is about 80 mm, so the average number of stop signals (detected scintillation photons) is not more than 0.1 per single excitation for the most luminous PWO scintillators. The count rate of the useful events (photons produced by scintillation decay in PWO) is 200–300 cps, and a decay spectrum with acceptable statistical accuracy can be acquired in 2–3 min. The expected improvement of the measurement productivity with a BaF_2 scintillator is by a factor of 2, and with multi-stop rejection by a further factor of 5.

To avoid variations of the useful-event count rate with time, energy scale stabilization systems (ESS) are being installed for both stop and start channels. Stop-channel ESS will automatically stabilize the position of the R5600 single-photoelectron peak position, and start-channel ESS will stabilize the position of the ^{22}Na 511 KeV photoabsorption peak. Briefly, ESS consists of a reference-voltage source, a variable-gain amplifier, a differential discriminator section with counters and DAC, the output of which controls the amplifier gain to minimize the difference between actual amplitudes of PM pulses and the reference voltage.

The TDC channel consists of a Time-to-Amplitude Converter (TAC) with 1 μs scale and a 1024-channel ADC providing 50 ps resolution. Start and stop inputs of TAC are driven by two

CFDs with less than 150 ps time walk. The ADC data are read by a PC (Pentium-100) through a CAMAC-PC controller for the time being.

4.2 Software

A software development platform of an IBM-compatible PC with Windows'95 operating system was chosen due to availability, low cost and ease of integration with a 3D machine control system. It has been implemented mainly on a PC platform. On the other hand, Windows'95 makes a possible transfer to the Windows NT operating system, which is foreseen as the platform for the C.R.I.S.T.A.L. project, without the need for a complete code change.

As designer software tools, Microsoft Visual C++ (a powerful environment allowing the creation of high-performance low-level software) and Microsoft Visual Basic (a convenient environment for rapidly creating high-level user-friendly data processing and presentation software) were chosen. Both of these tools are supported by the CERN Computing Division.

The implemented software can be divided in four layers:

- L-1. Low-level hardware drivers. Currently this is a CAMAC driver, oriented to a FK4410 PC-CAMAC interface and implemented as a Virtual Device Driver (VxD).
- L-2. Device drivers which control specific device modules through driver L-1 and also provide data conversion between levels L-1 and L-3. Implemented as several VxDs.
- L-3. Dynamic problem-oriented libraries, providing the interface between VxDs and high-level software L-4 written in Visual Basic. Implemented as several DLLs.
- L-4. High-level application software which provides data processing, presentation, user interface, etc. Implemented as several EXE modules.

Such a software structure allows complete software re-engineering to be avoided, when a new hardware or a new OS is used. As an example, when Windows '95 is replaced by Windows NT, only the L-1 and L-2 drivers have to be changed. If the CAMAC standard is changed to VME as foreseen for the final ACCOS, only L-2 should need to be completely rewritten; and some modification may be needed to L-3 and the new L-1 driver usually supplied with the PC-VME interface.

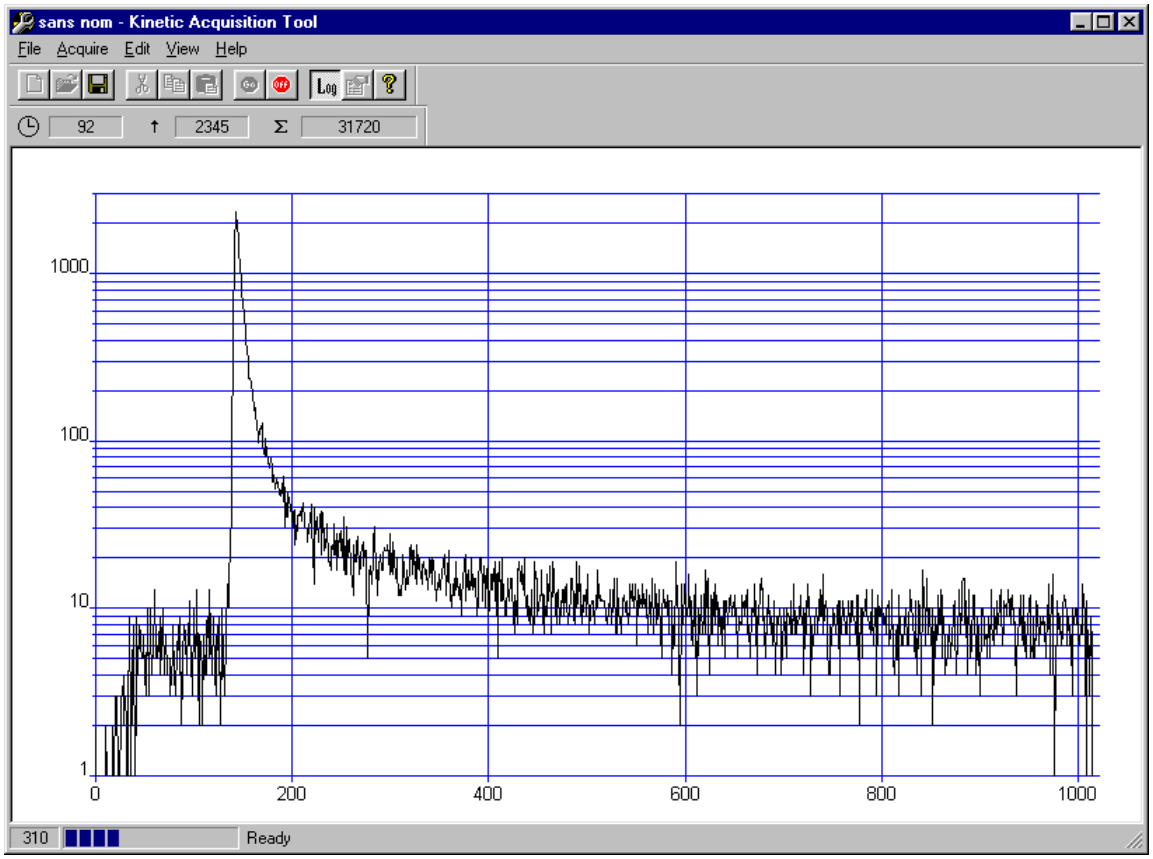

Fig. 6: Sample screen of the Kinetic Data Acquisition module.

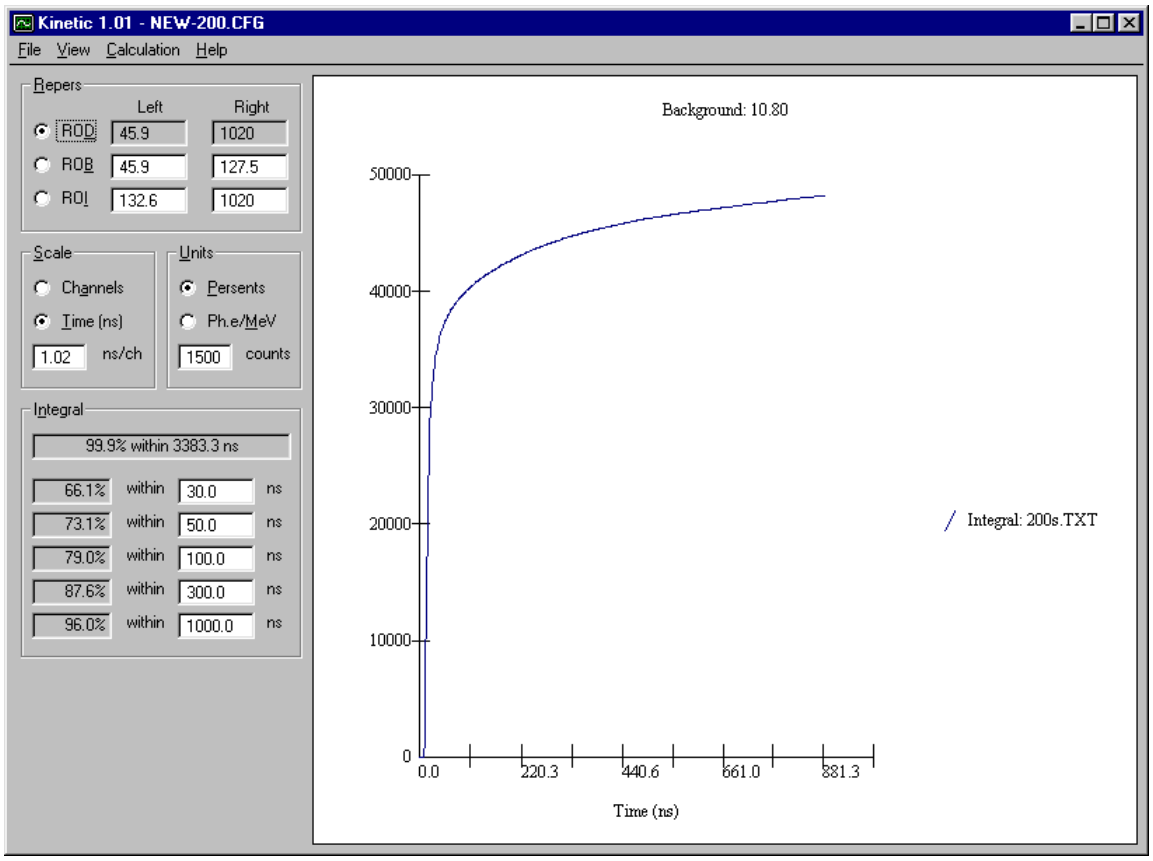

Fig. 7: Sample screen of the Kinetic Data Processing module.

4.3 Schedule and cost

A standard 3D machine (see Appendix 4) is foreseen for use in the ACCOS system. Most of the electronics of the measuring modules are available in the VME standard. The other system parts, designed and developed by us, such as crystal server, ESS, spectrophotometers, are in the testing and evaluation process. An order for production could be placed in optical and mechanical factories during the course of 1997.

At present, the estimation of the overall cost according to the elements detailed in Appendix 4 amounts to 199 830 CHF, in full agreement with the cost book (version 8) published in February 1997. This estimation includes both transverse and longitudinal measurement facilities for the optical parameter measurement, and the price of an extra CPU.

Appendix 1

Algorithms of data correction and calibration

A.1 Optical transmission measurements:

Reconstruction of the longitudinal and transverse transmission non-uniformities and calculation of the light attenuation length.

The averaged absorption coefficient, obtained from transversal measurements, can be determined as

$$\langle \mathbf{k_i} \rangle = \frac{\Sigma\left[\mathbf{k_m}(\lambda_i)\right]}{\mathbf{m}} \ . \qquad (1)$$

with m labelling the different measurements along the crystal.

Using equation (1), the longitudinal transmission of the crystal will be

$$\mathbf{T}(\lambda_i) = [1 - \mathbf{r}(\lambda_i)]^2 \ \mathbf{e}^{- <\mathbf{k}(\lambda_i)> \ l} \ ,$$

where l is the length of the crystal, $\mathbf{T}(\lambda_i)$ is the longitudinal transmission (LT) of the crystal at λ_i, and $\mathbf{r}(\lambda_i)$ is a constant at the specific wavelength.

Transversal transmission non-uniformity at the selected wavelength (i.e. 500 nm) is determined as

$$(\mathbf{T_m} - \mathbf{T_{max}}) / \mathbf{T_{max}} = \mathbf{e}^{\beta} - \mathbf{1} \ ,$$

where

$$\beta = - (\mathbf{k_m}^{(\lambda = 500)} - \mathbf{k_{max}}^{(\lambda = 500)}) \ .$$

The light attenuation length is determined as

$$\mathbf{L}^{(\lambda = 500)} = \mathbf{1} / < \mathbf{k}^{(\lambda = 500)} > \ .$$

Here, we estimate the systematic and the stochastic errors of the method. As an example, let us consider the procedure of longitudinal transmission reconstruction by transversal measurement. The digitized values are reference amplitudes, information amplitude and dark signals $\mathbf{I_{ref}}(\lambda)$, $\mathbf{I_{inf}}(\lambda)$, $\mathbf{I_{dark}}$. Then, the value of transversal transmission (TT) at the specific wavelength is calculated:

$$\mathbf{T} = (\mathbf{I_{inf}} - \mathbf{I_{dark}}) / (\mathbf{I_{ref}} - \mathbf{I_{dark}}) \ .$$

For λ = 500 nm, the value of $\mathbf{I_{ref}}$ is about 200 nA, and $\mathbf{I_{dark}}$ of the PD is 1 nA. While the expected measurement time is 10 seconds, the pulse-height distributions of $\mathbf{I_{ref}}(\lambda)$, $\mathbf{I_{inf}}(\lambda)$, $\mathbf{I_{ref}}(\lambda) - \mathbf{I_{dark}}$ consist of about 500 events for each specific wavelength. Therefore, the problem becomes precise determination of peak position rather than of transverse transmission. Taking into account that the distributions mentioned above will be narrow enough (roughly 1% FWHM), the peak position can be found with an accuracy of at least 0.1 %.

On the other hand, the intensity of light passing through the crystal can be expressed as

$$\mathbf{I = I_0 (1 - r)^2 \times e^{-(l/L)} + I_0 (1 - r)^2 r^2 \times e^{-(2l/L)} + ...}$$

The value of **r** for PWO at 500 nm is about 0.14 and depends on the refractive index and on the crystal surface roughness; therefore, it can not be taken as constant at the defined wavelength. In practice, the $\mathbf{(1 - r)^2}$ multiplier can vary by up to 3% due to surface state even for normal optical polishing, which means that this systematic error dominates in transmission measurements at least in the visible region. One can calculate the influence of errors in TT measurements on the reconstructed LT value. Table 1 shows how a 1% deviation of TT influences LT at two wavelengths:

l (nm)	400			500		
Transversal transmission (%) measured on 2 cm	64	65	66	71	72	73
Longitudinal transmission (%) reconstructed for 23 cm	18.7	22.4	26.7	50.5	57.7	67.6

Table 1. Errors in reconstructed longitudinal transmission.

One can see that even a 1% error in TT leads to ~15% error in LT. If we assume 3% error for TT we can obtain values for LT greater than the theoretical value, which are meaningless.

For the short-wave PWO transmission, the decrease of the signal levels because of the halogen-lamp emission spectrum shape leads to an increase in the stochastic error. From the other hand, due to of stronger absorption in PWO, systematic error caused by uncertainty in reflection decreases. So in the UV and blue region the stochastic error dominates. An increase in the stochastic error is roughly offset by the decrease of the attenuation length **L** at these wavelengths (for instance, measurable limit for **L** will be 1 m, while typically **L** = 0.1 m). Moreover, in case of strong absorption of the UV light (especially in the 300–350 nm range), transversal measurements can provide even better accuracy than direct measurement of longitudinal transmission of a 23 cm long crystal.

A.2 Decay time curve processing:

Corrections for the instrumental factors.

A.2.1 Source decay

As a ^{22}Na annihilation source is used in measurements, the problem of source decay arises. According to our estimations, the source intensity would have to be at least 200–300 kBq to provide acceptable measurement productivity. Because of the relatively short half-life of ^{22}Na (about 2.7 years), after 3–4 years the source should be replaced. One possible solution is the use of a **^{44}Ti** source (its availability is under study). Source decay will influence LY and LYN data because of a change of the photon count rate with time. There are two ways to overcome this problem. The simplest is to follow in the ACCOS computer the current intensity of the source, since the date of production and half-life are known. Because the radioactive source is mechanically connected with the start detector, and the start channel is stabilized, a change of the start channel count-rate will be

due to the source decay only. The second way is to measure the count rate in the start channel. This count rate will go to a scaler which can be read by a data-processing computer program.

A.2.2 Dead-time losses and distortion

According to [5], the probability **W** of detecting a scintillation photon in a TDC channel ***i*** measured by the delayed coincidence method with a one-hit TDC is given by

$$W_i \sim c_i /(1 - g) - \lambda_i \Delta t_i N ,$$

where c_i is the channel content; Δt_i the width of the ***i***-channel of TDC; **N** the total number of measurement cycles (number of starts); λ_i the noise-event flow (random coincidences between start and stop channels, PM dark current); $g = (c_1 + c_2 + ... + c_i) / N$, i.e. dependent on signal plus noise flow. (It is assumed that these flows have a Poisson distribution.)

In the case where $g << 1$, this means low signal-plus-noise flow, the measured time spectrum is not distorted (practically, for $g \leq 0.1$). For $g > 0.1$, significant spectrum shape distortion will take place for large numbers of ***i***. In practice, a conventional one-hit TDC digitizes the arrival time of the first stop pulse after excitation. Dead time of such a TDC does not allow more than one time interval per single excitation to be digitized. Therefore, the presence of events having more than one 'stop' pulse per 'start' will bias acquired data (later occurring 'stops' will not be measured with the same probability). With the increase of the channel number, the systematic error and the size of the correction needed will grow. This bias can be corrected mathematically in principle, but only in the case where a single source of distortion is present. Unfortunately this is not the case for PWO, because its fast scintillation component is comparable with stop-channel dead time, which leads to uncertainty in **g**-calculation.

One-hit TDCs with a 'multi-stop' rejection circuit can determine whether more than one stop signal arrives in the sampling period after the start pulse. Here, events with more than one stop signal per start are rejected, and W_i is

$$W_i \sim c_i - \lambda_i \Delta t_i (N_0 - N_0 N_2 / N_1 + N_1 / 2) ,$$

where N_0 is the number of measurement cycles without stop pulses within the sampling period,
N_1 the number of measurement cycles with a single stop signal,
N_2 the number of measurement cycles with two or more stop signals.

One can see that there is no spectrum distortion dependent on the channel number. The flat background of noise events can be determined and subtracted. In this method, an increase in the average number of detected stop pulses per single excitation over a value of about 0.1 results in an increase in the dead time and, furthermore, in a decrease in the measurement productivity [4]; so, there is an optimal count rate for a stop channel. However, the optimal value corresponds to a productivity rate 10–20 times greater than with the conventional method. The dead-time losses, which are considerable for LY measurement based on decay-curve integration, can be calculated using TDC 'dead time' output.

Some modern 'multi-hit' TDCs are capable of measuring the arrival times of q stop pulses per single start. Empirically, the increase of productivity is $\varepsilon \approx 3q/4$ for $q \geq 2$. However, it is useless if the stop channel dead time is of the same order of magnitude as the fast scintillation components.

As a conclusion, the most adequate TDC for the PWO scintillation decay measurements is a one-hit type with multi-stop rejection unit. The results of the system prototype tests with a conventional one-hit TDC show that a one-hit TDC provides a measurement time of about 100 s per point. Applying 'multi-stop' rejection will provide acceptable accuracy and productivity of ACCOS measurements (about 20 s per point), with a gain factor of 2 if a BaF_2 scintillator in used for the start channel instead of a plastic one. This gives an overall factor of 10, which is achievable for the final version, allowing a start stop measurement duration of < 4 min for one crystal.

A.3 LY uniformity curve processing:

Correction for deposited energy and spatial function of excitation
Correction for solid angle, visible by 'stop' photodetector
Correction for the difference in absorption length visible by PM and APD

The geometrical model used for mathematical modelling of LY uniformity measurement is shown in Fig. 3.

The mathematical basis for modelling is as follows. The PWO crystal is irradiated with a low energy gamma-quantum or a stopping proton source (like the one used in PSI). In the case of gamma quanta, the crystal absorbs part of gamma-quantum energy due to Compton scattering. Some part of gamma-quantum energy can leave the crystal, i.e. by scattered gamma quanta. In the protons case, the full energy is deposited in the crystal. A part of the energy deposited by gamma quanta or protons is converted into the energy of light photons visible by a PM. The PM response **I(z)** is then given by integration on the crystal volume v :

$$\mathbf{I(z) = a \times \int_v G(z, z', r_\perp, E_\gamma) \times P(z, z', r_\perp)\, dz'\, dr'\,,}$$

where $\mathbf{G(z, z', r_\perp, E_\gamma)}$ is a function of gamma-quantum energy deposition in the elementary scintillator volume where the initial energy is $\mathbf{E_\gamma}$ and the coordinate of radioactive source is **z**. This function also depends on non-indicated parameters such as crystal size and shape, physical and chemical structure of the crystal and on the source trajectory.

$\mathbf{P(z, z', r_\perp)}$ is the probability of detecting an optical photon by a PM when it is emitted from point **z'**. This function also depends on boundary conditions on the crystal sides and on the optical coupling between crystal and PM. If the dependence on transversal coordinates $\mathbf{r_\perp}$ is weak, then for fixed Eγ

$$\mathbf{I(z) = a \times \int G(z, z') \times P(z')\, dz'}\,.$$

If the 'ideal' experiment on LY uniformity measurement is a proton beam experiment with point-like excitation along a crystal axis **z**, then

$$\mathbf{G(z, z') \cong G_0(z) \times \delta(z - z')},$$

and the PM response is

$$\mathbf{I_p(z) \cong G_0(z) \times P(z)}.$$

While the gamma quanta are used for crystal excitation, **G(z, z')** is a more complicated function and the integral equation as mentioned above has to be solved to find LY at the given **z** point and to reconstruct the LY non-uniformity curve.

One should note that, generally, the **P(z)** function is also different in proton and in gamma-quantum experiments. This is due to the different conditions of crystal to PM optical coupling in the two types of measurements. So, the problem of modelling consists of two parts: a nuclear one and an optical one.

The modeling of the nuclear part is performed by the EGS4 computer program [6]. The gamma quanta are emitted isotropically from a source point. According to the ^{22}Na spectrum, either a photon with a 0.511 MeV energy and a probability of 0.5 is emitted in the upper semi-sphere (2π solid angle), or a 1.23 MeV photon is emitted in 4π with the same probability (a pair of 0.511 MeV annihilation quanta are emitted in opposite directions, so only one of them can enter the crystal).

Each quantum is considered by the program either before it is completely absorbed, or before it has reached the crystal boundary. Coordinates of each interaction and the deposited energy are calculated. Using this information, the **G(z, z')** is restored. $PbWO_4$ (chemical formula) was used for these simulations, the crystal density was taken as 8.28 g x cm^{-3} and γ-energy threshold of 40 KeV have been used.

The main results of simulation are:

$$\mathbf{G(z, z') = (2AW/\pi) [1/(W^2 + 4(z - z')^2] ,}$$

with **A** = 0.22 m, and **W** = 2.1 m for a tapered crystal, used in test.

For optical-response simulation, geometrical optics and Monte Carlo method were used. From the random point inside the crystal, a light beam was emitted. Taking into account geometrical optics rules, absorption and boundary conditions, the beam history was simulated before the beam was absorbed, escaped from the crystal, or reached the PM window. The boundary conditions are:

a) Side surfaces: refraction according to Fresnel's formulas, Lambert law (**I ~ cos** β) for wrapping (if present).
b) Crystal top: mirror reflection.
c) Crystal bottom: Fresnel's formulas.

The relation between the proton case with an APD $\mathbf{P_p(z)}$ and the gamma case **P(z)** is

$$\mathbf{P(z) = C\ (z_0+b)^2/\ (z_0 - b)^2 exp\ (\alpha_{eff}\ z)\ S(z)\ P_p(z)\ ,}$$

where $\mathbf{z_0}$ and **b** are constants, dependent on the geometry of the crystal and of the light collection on the stop PM and APD, $\alpha_{\mathbf{eff}}$ is the effective difference between light-absorption coefficients visible by PM and APD, derived from longitudinal-transmission measurements, and **S(z)** is the additional correction for non uniformity of $\alpha_{\mathbf{eff}}$, derived from transversal-transmission measurements.

Appendix 2

Decay time and light yield measurement – Results

The main results of the start-stop method using a ^{22}Na source with a plastic scintillator (start), as described in paragraph 3.1c and in Appendix 1, are presented. The main correction curve due to the Compton energy escaping from the crystal is shown in Fig. A2-1. It was determined for the test geometry used.

The relative light yields for three crystals, also measured with protons at PSI, are presented in Figs A2-2 to A2-4 and compared to the PSI results. All curves have been normalized to the point recorded at 8 cm from the photomultiplier. The same correction function was applied to all of them and the good agreement shows that the start-stop method proposed for ACCOS is able to provide the relative LY and the LYN, as stated, in addition to the decay time of the crystal (Figs 6 and 7).

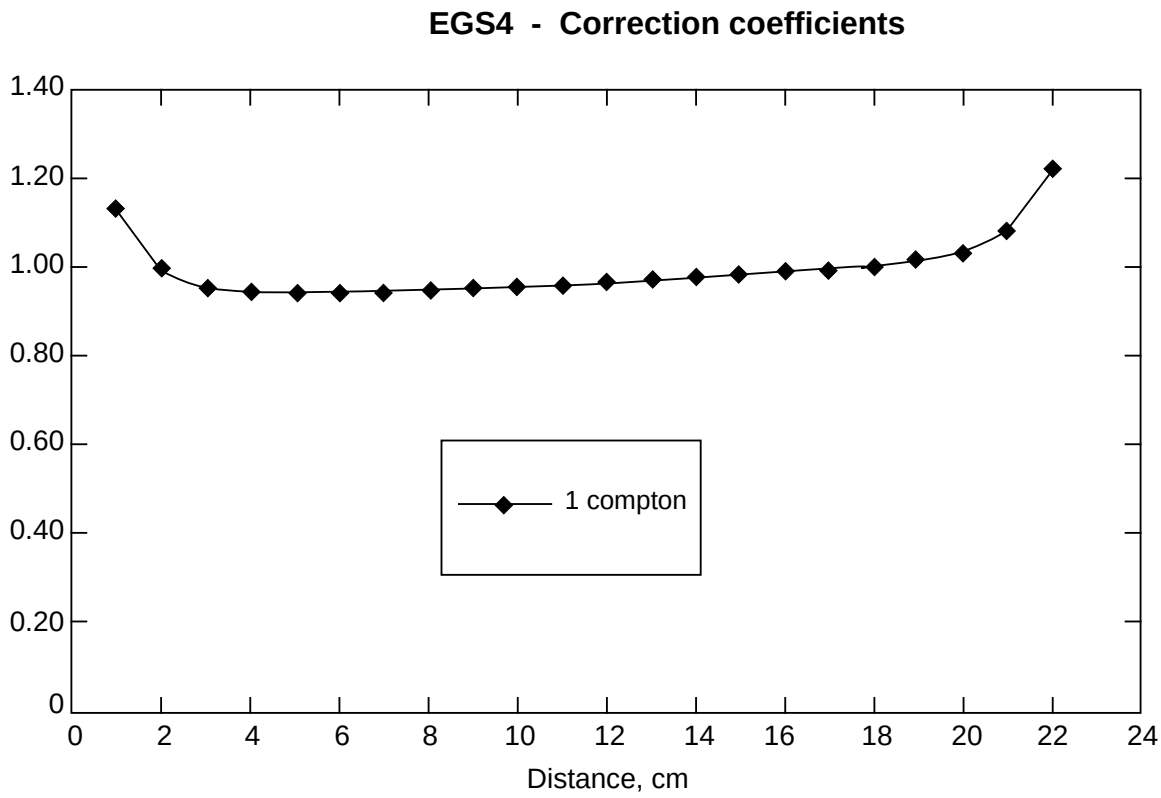

Fig. A2- 1 Correction for energy leakage for full size tapered PWO crystal E_γ = 511keV.

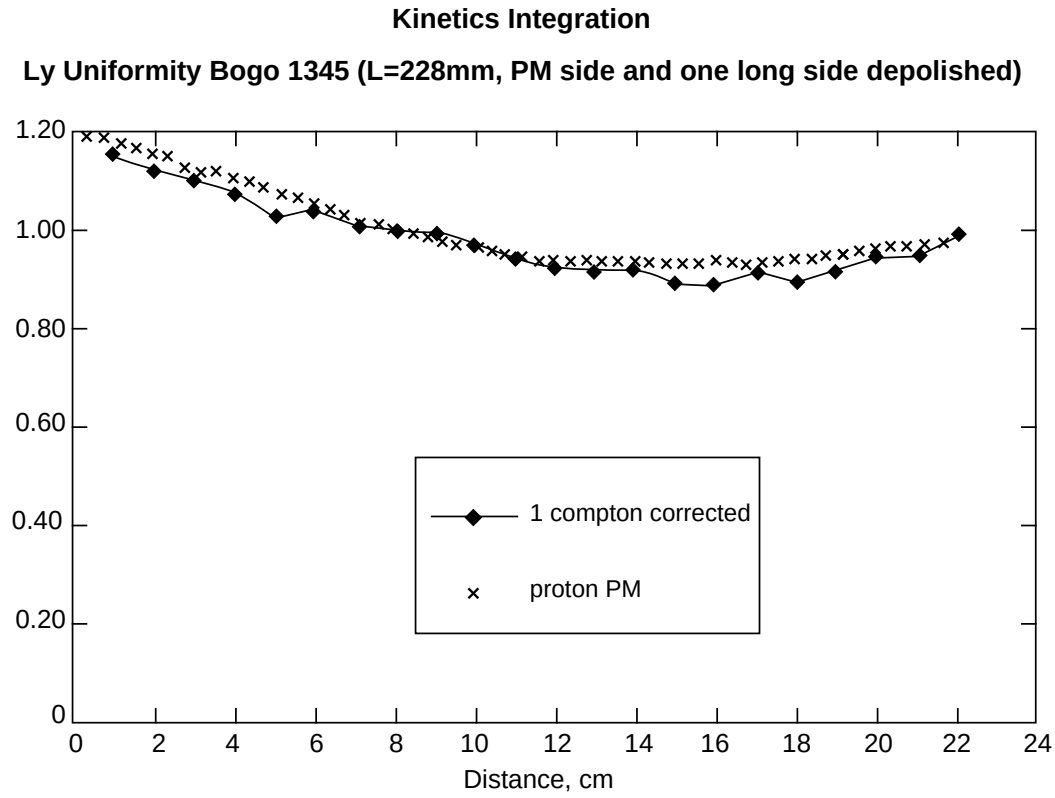

Fig. A2- 2 INP (Minsk), LAPP

Kinetics Integration

Ly Uniformity Bogo 1333 (L=230mm, PM side and one long side depolished)

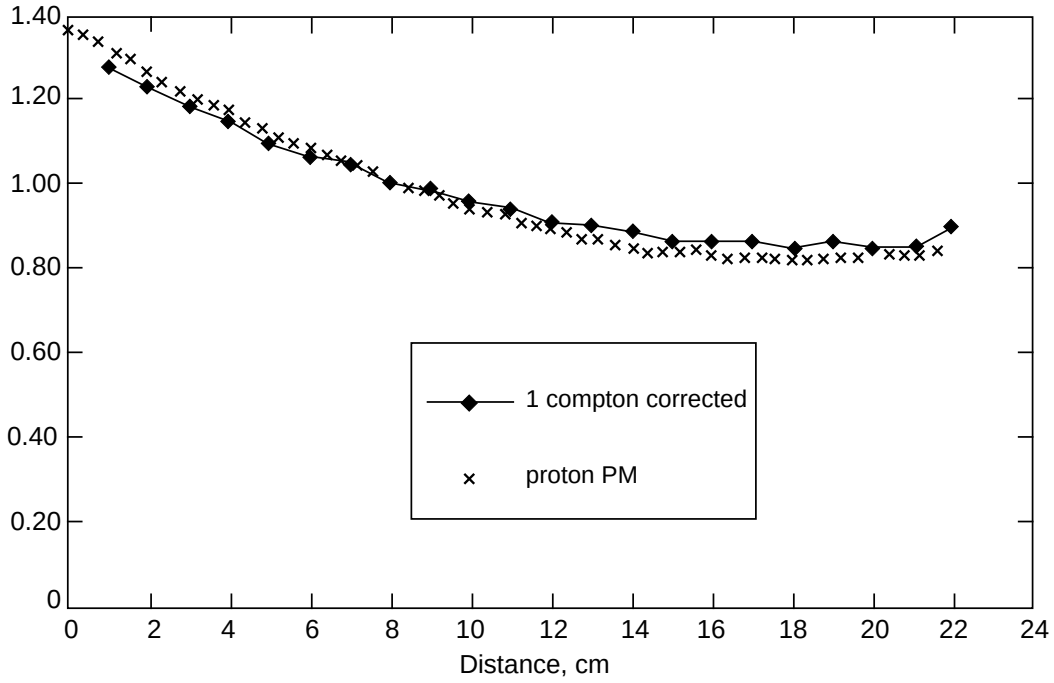

Fig. A2- 3 INP (Minsk), LAPP

Kinetics Integration

Ly Uniformity Bogo 1347 (L=230mm, PM side grinded, one long side slightly depolished)

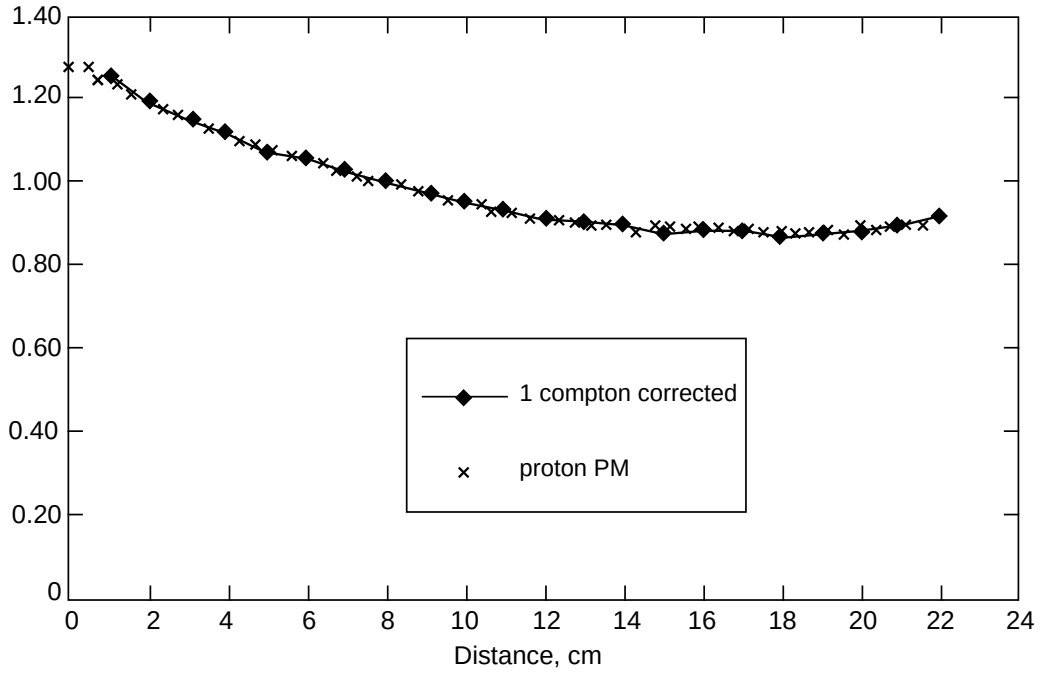

Fig. A2- 4 INP (Minsk), LAPP

Appendix 3

Transmission measurement on OS-1 – Results

Transversal measurements were done on a series of different crystals of various types to show the ability to reconstruct the short-wavelength absorption slope, to put in evidence absorption band like the 420 nm one, and to detect diffusing internal structures which could be present in the crystal. This is illustrated in Figs. A3-1 to A3-6. In particular, Fig. A3-1 shows the detection of a smoky cloud close to the beginning of the crystal near the photodetector.

The overall time required to measure the 11 points along the crystal and 11 wavelengths per point is only three minutes.

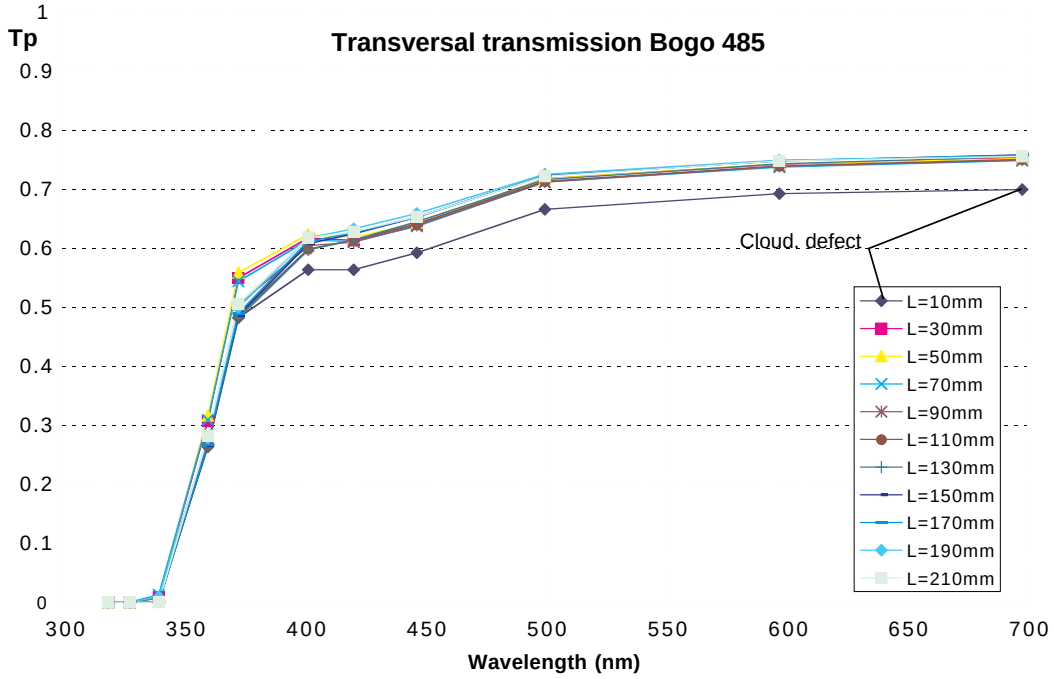

Fig. A3-1 INP (Minsk), LAPP

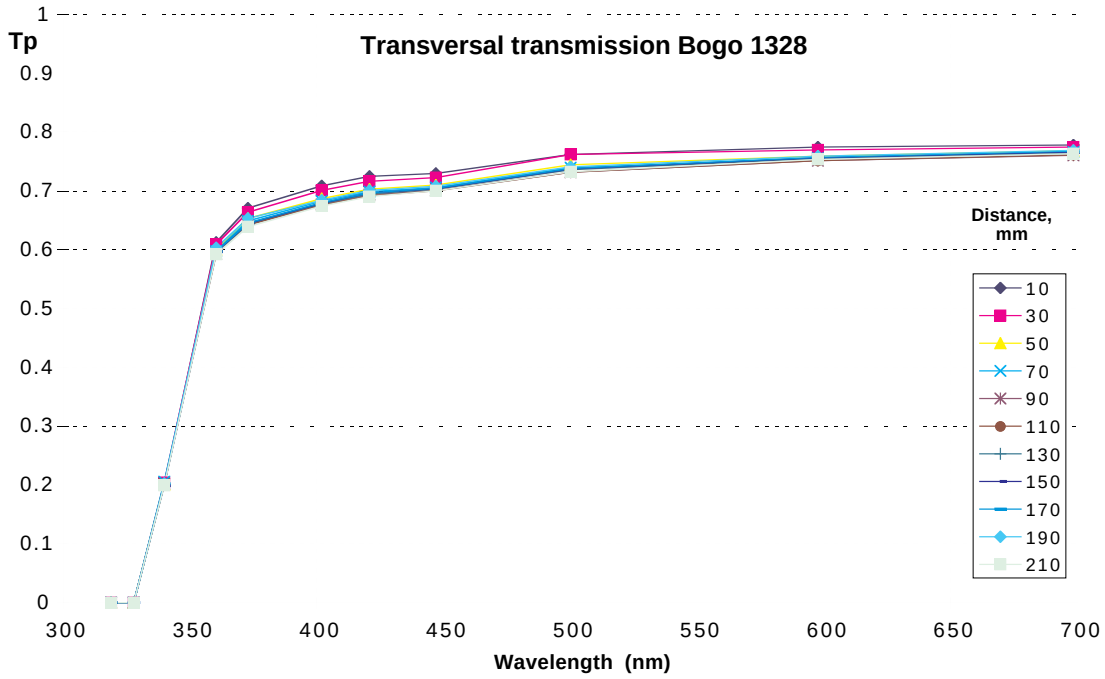

Fig. A3-2 INP (Minsk), LAPP

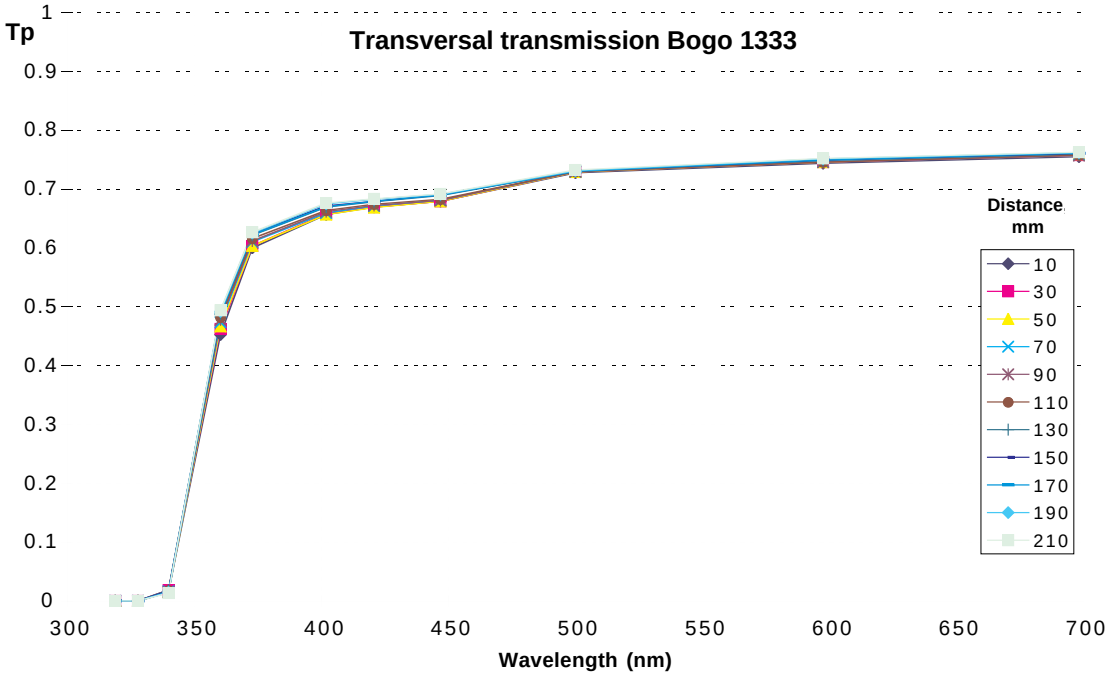

Fig. A3-3 INP (Minsk), LAPP

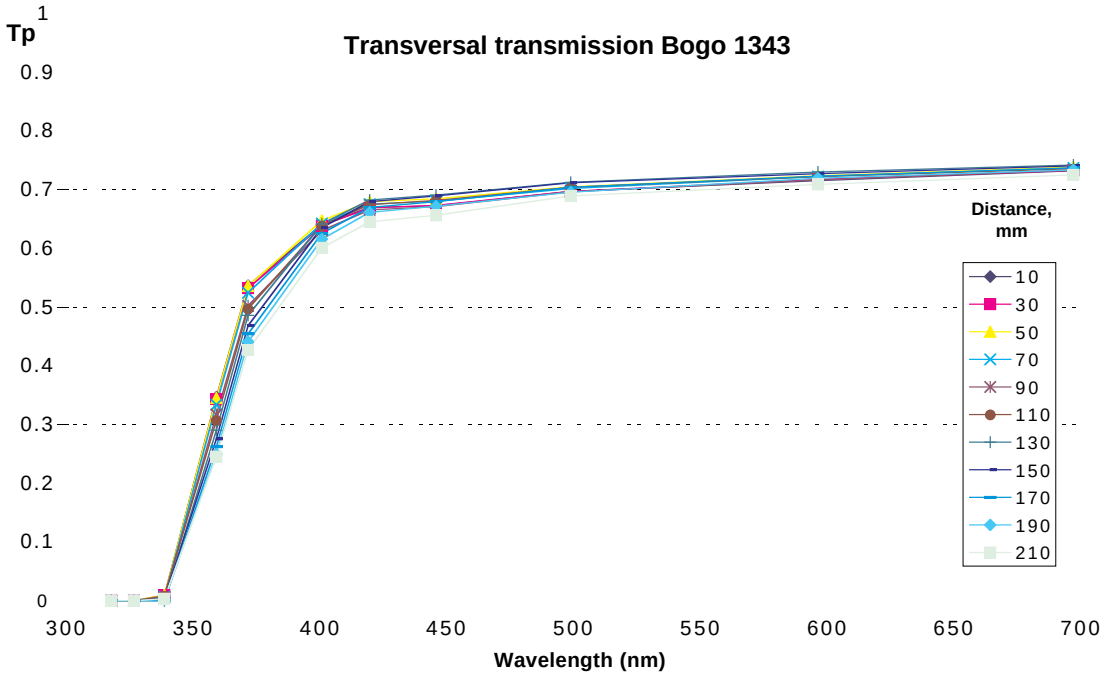

Fig. A3-4 INP (Minsk), LAPP

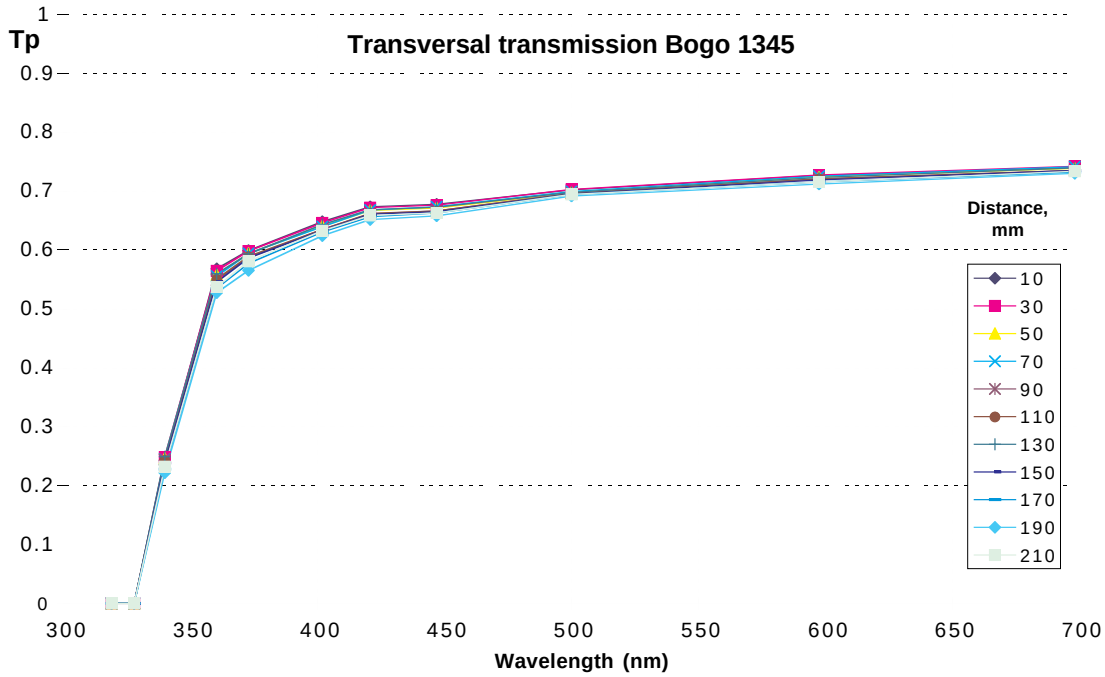

Fig. A3-5 INP (Minsk), LAPP

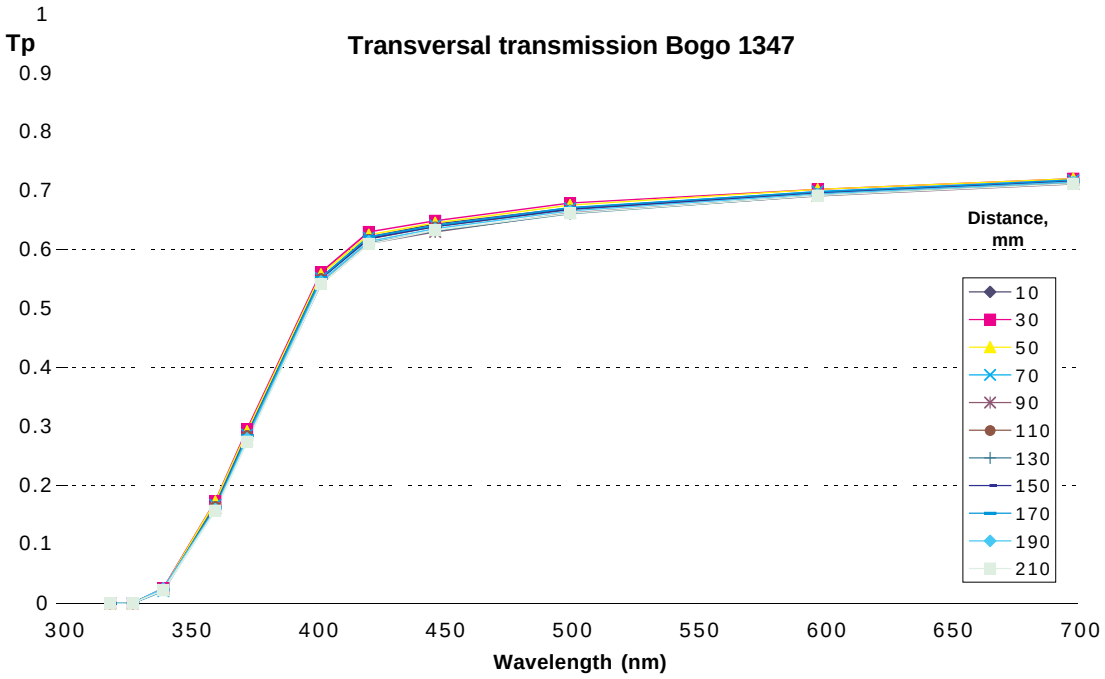

Fig. A3-6 INP (Minsk), LAPP

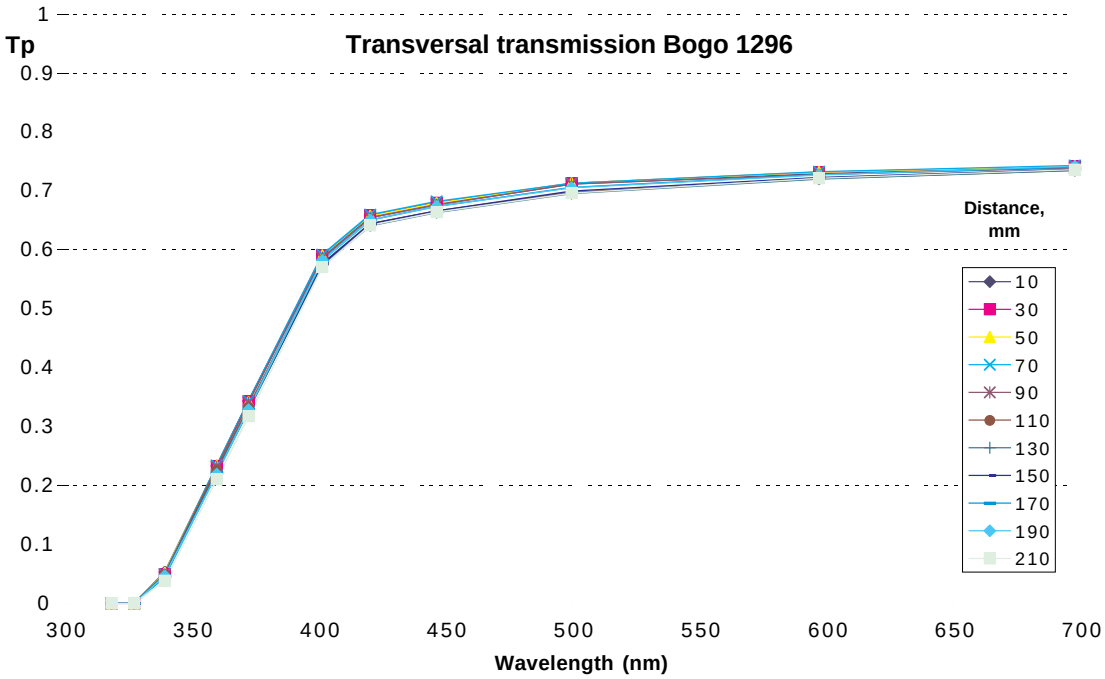

Fig. A3-7 INP (Minsk), LAPP

Appendix 4

Crystal dimension measurements and mechanical installations. Some policy considerations

Dimension measurements and mechanical installations

Constructors throughout Europe were contacted (around 80) with a proposition including a rotating server and its movement. Eight companies gave a satisfactory answer to our request. In alphabetical order, they are: CORD, DEA-TESA, JOHANSSON, LK, MITUTOYO, POLI, TRI-MESURE and ZEISS.

Figure A4-1 (A to D) shows the different arrangements which have been considered to achieve fully or semi-automatic versions of an ACCOS system. The semi-automatic arrangement achieved by separating completely dimension and optical measurements is shown for completeness. In this case, the prototyping concerns only the measurement of the optical parameters. All 3D machines can fulfil the B, C, and D arrangements but only two were found to fit with the A configuration. A and D arrangements are able to process up to 20 crystals, but A is able to do it with a 1 m diameter rotating server, whereas for D a rotating server of 1250 cm must be used. Moreover, the price of a rotating server would be significantly higher for D, as it cannot be driven by a simple central motor but requires a more elaborate mechanism with some type of notched crown wheel and must be dismantled in several pieces for installation. The B geometry can be accommodated by any kind of machine, but the treatment is limited to seven or eight crystals for two reasons:

- the choice of the small portico machine shown, cheeper than the machine fitting the A solution,
- the price of a linear movement even of moderate dimensions to keep the system fully automatic (such a system is rather expensive even if built from off-the-shelf components).

In our view, solution A has definite advantages over solutions B, C and D. In a smaller volume, more crystal can be treated in an automatic way. The rotating server can be delivered by the constructor of the 3D machine and only one bar-code reader is needed (in solution C where automatic sequencing between geometrical and optical measurements are decoupled, two are needed).

From our investigations of the european market, two machines have been proposed with an open geometry and with an attractive price, one provided by JOHANSSON and the other by POLI.

The basic prices of these machines, including the standard software and without server, are 81 330 CHF and 85 678 CHF for JOHANSSON and POLI respectively. The evaluation for the rotating server is: 18 414 CHF and 30 946 CHF respectively.

To equip these machines with the movements foreseen for the optical measurements as described in this report, at least one two-axis movement is needed with its software. Such an item is available on the market. An expense of 16 000 CHF has to be foreseen (PARKER). The cost of the mandatory bar-code reader for crystal identification before or during measurement has been calculated at 3 370 CHF, including its interface as well as decoding and driving software (KEYENCE).

Figures A4-2 and A4-3 outline the design of a insulated measurement cabin which is equipped with two loading and unloading chambers. The cabin, which is installed in a room kept at a roughly constant temperature, can be easily stabilized in temperature to 0.1°C and maintained in the dark. Around 10 000 CHF have to be added for such a construction equipped with air conditioning.

Optical detection devices are based on series 5600 and 5900 Hamamatsu PMs; 3 000 CHF must be added for the detectors themselves and 10 000 CHF for the specific associated electronics. The spectrophotometer proposed by the Minsk institute for the transversal transmission measurement can be estimated to 22 500 CHF and a longitudinal transmission spectrometer can be built for the same or a lower price. Outside our investigation, a Czech company, BMD, has proposed a small closed-geometry machine with a linear or circular movement of the crystals (see Table A4-2).

Some policy considerations

In view of the integrated instrument as proposed here, problems of warranties and software access must be considered before a final choice is made. For warranty reasons and to avoid any dispute in case of malfunction in the future, it is highly desirable that the rotating server is provided by the 3D machine company under its own responsibility and warranty. In comparison, the price of a rotating server provided separately would be at least as high. This formed part of our request during our investigations. Most of the companies provide standard software to operate predetermined situations, but not all are ready to give free access to their software to communicate with it, in case of integration in a higher software program which has to decide the overall sequences of measurement (geometrical, optical, and both in various sequences). Some of them propose an additional licence cost for each new adaptation. Even if in the standard situation, at least at the production level, the sequence remained largely unchanged, a more flexible situation has to be foreseen for the regional centres.

The best case would be if only one PC work-station or similar could be used for all the control of the combined machine. However, if the availability and technical performance considerations impose two different systems, provided that they are able to communicate, the cost increase will be limited to 4 000 CHF which corresponds to the cost of an independent PC work-station for the identification and optical parameter handling.

All the above considerations assume an automatic bench which can integrate the essential functions of control which could be accepted by a large number of actors (producers and regional centres) in order to minimize cost and to unify methods and material as much as possible, which would improve speed and cost of maintenance in case of failure as well as provide a worldwide after-sales service. Other independent benches for optical measurement can be built or bought and operated together or separately, each one as an independent instrument being equipped with a bar-code reader to identify properly the crystal under treatment. Dimension measurement can be completely decoupled from the optical measurements and considered as an individual instrument connected directly to the CRISTAL system and used alternatively for different metrology tasks: crystals, alveola or other tasks. Nevertheless, arguments put forward to separate the dimension measurement machine from the optical benches are not fully justified, because the total time needed for any complete parameter measurement of one crystal: dimensions, transmission, LY by start stop method (with the efficiency gain due to the use of a BaF_2 start channel and of a multi-hit rejection TDC) is below ten minutes. This allows to proceed to the treatment of 60 crystals in 12h, (including loading and unloading times), leaving 12h a day for other metrology tasks. Taking into account that an automatic machine should be able to operate for a large part of the night without human intervention (except for loading and unloading) this surely leaves 8h which can be dedicated to metrology tasks besides crystal treatment. Special access to the reference basis of the 3D machine can be easily foreseen through the rotating server in order to provide a strong basis for extra metrology tasks if needed.

Table A4-1 summarizes the overall cost of the proposition of this report. Table A4-2 summarizes the information provided by the eight constructors and the last column summarizes the BMD proposal.

Table A4-1[1]

ITEMS	ESTIMATED PRICES FS
3D machine	81 330
Rotating server	18 000
Start-stop movement	16 000
PM start-stop	3 000
PM associated detector	10 000
Bar-code + electronics	3 370
Air-conditioned cabin	10 000
Transverse transmission spectrometer	22 500
Longitudinal-transmission spectrometer	22 500
CCD smoky structure detector	3 000[2]
Extra PC unit	4 000
	193 700

NB: The mean working hour cost in European industries[3] can be estimated to be in the range 19.18 CHF to 31.965 CHF. For a non-automatic machine, 8 man/h of intervention per day will result in a five year period of 300 working days per year, at an extra cost of 368 000 CHF.

[1] Estimation within 10% made for four machines + a prototype; could be rediscussed inside an official call for tenders.

[2] Only mandatory at the production centres to eliminate unacceptable crystals with too many smoky or milky structures inside.

[3] Eurostat, Studies on the labour cost of labour 1988–1992.

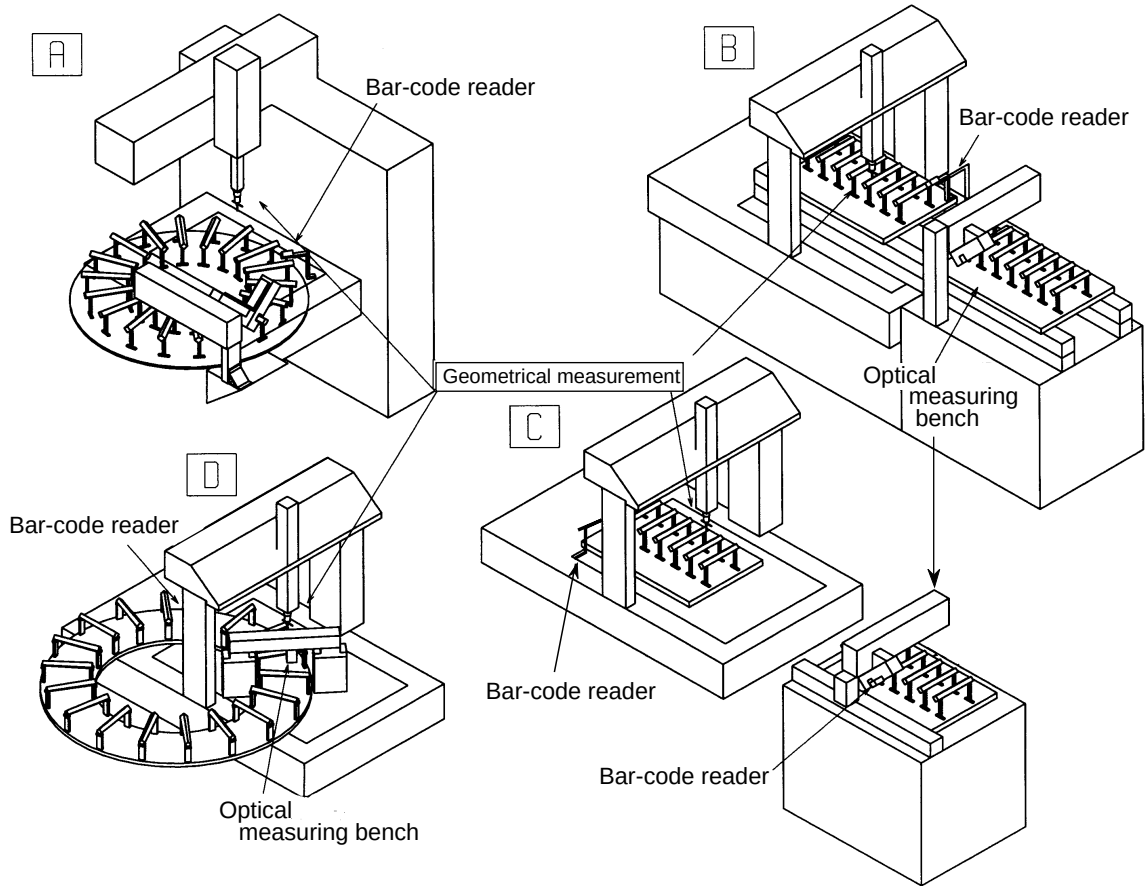

Fig. A4- 1 Arrangements for automatic A,B,D and semi-automatic C geometry.

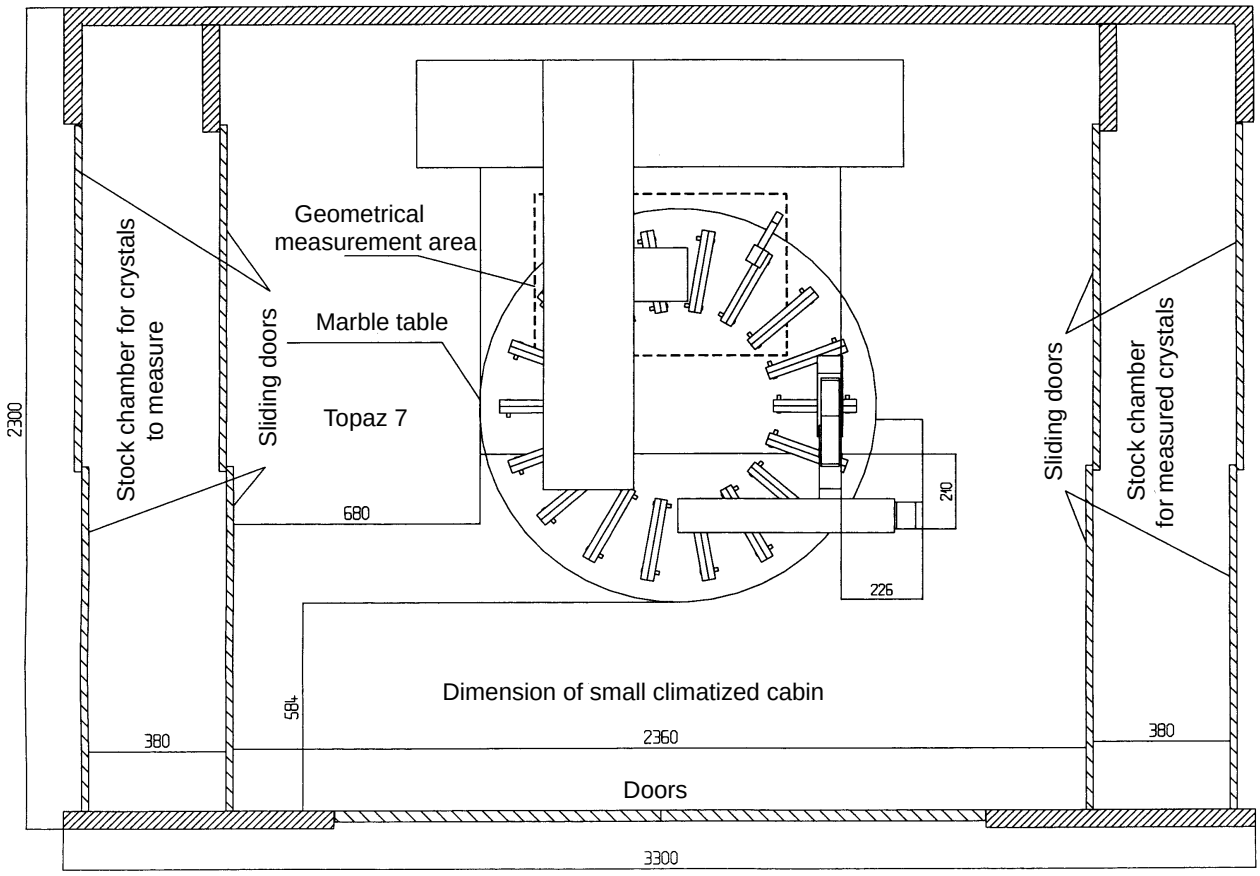

Fig. A4- 2 Design of measurement cabin : geometry A

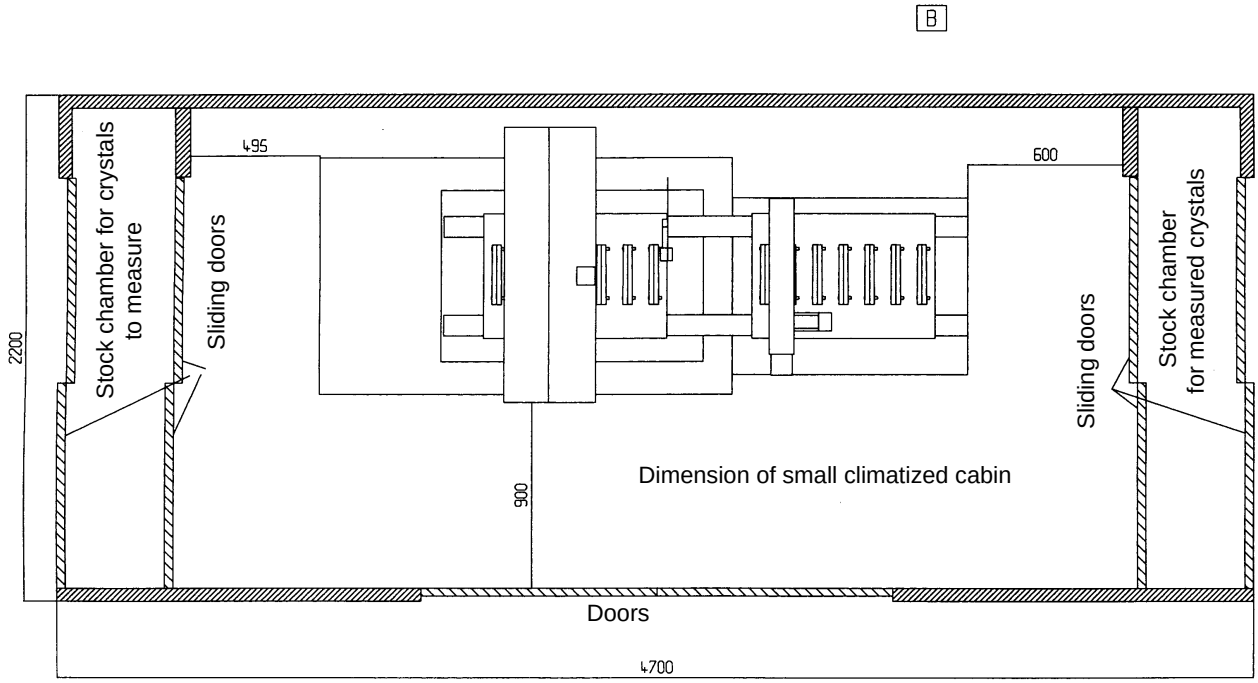

Fig. A4- 3 Design of insulated measurement cabin : geometry B

Table A4-2 **Technical and Financial Study for 3D-Machines**

	Mitutoyo	Tri–Mesure	LK	Dea–Tesa	Cord	Johans-son	Poli	Zeiss	Bmd
Capacity **X**	700	700	600	1000	1000	700	400	700	400
mm **Y**	600	400	500	700	550	450	400	700	600
Z	400	400	400	500	400	450	400	500	350
Machine	98465	111637	94629	97188	84910	81330	85678	137596	75985
Rotating Server **A**	No	No	No	No	No	26854 then 18414	30946	No	10546
A						14322	14322		
Option **B**	28465	28465	28465	28465	28465			28465	
C	27442	27442	27442	27442	27442			27442	
Cristal Holder Tray **B-C**	3836	3836	3836	3836	3836			3836	5359
Training	Included	3836	Included	4795/pers	2711	3453	12788	8586	
Delivery and put into operation	Included	Included	Included	1151	3069	Included	7673		Extra Cost
TOTAL SF/HT A						125954 or 117519	151407		86531
TOTAL SF/HT B	130767	147775	126931	135435	122992			178465	
TOTAL SF/HT C	129744	146752	125908	135435	121969			177442	81344

Change evaluation at 31/1/97

References

[1] M.Lebeau et al., A distributed control and data base system for the production of high quality crystals, CMS/TN/95-024.
J.-M.Le Goff et al., A data capture and production management tool for the assembly and construction of the CMS ECAL detector, CMS Note 1996/003.

[2] I.Dafinei et al., Lead tungstate for high energy calorimetry, Mat. Res. Soc. Symp. vol. 348, 1994, p. 99.

[3] A.Zaidel, Technika i practica spectroskopii, Moskow, Nauka, 1966, p. 386.

[4] W.W.Moses, A method to increase optical timing spectra measurement rates using a multi-hit TDC, NIM A 336 (1993) 253-261.

[5] A.F.Cherniavskii, S.V.Beketov, A.V.Potapov, Statisticheskie metody analiza sluchainyh signalov v iaderno-fizicheskom experimente, Pod. red. A.N.Pisarevskogo, M., Atomizdat, 1974, p. 352.

[6] W.R.Nelson, H.Hirayama, D.W.O.Rogers, The EGS4 CODE system, SLAC report-265, 1985.